Characteristics of $BaTiO_3$ Particles Prepared by Spray−Coprecipitation Method Using Titanium Acylate-Based Precursors

Guang J. Choi,* Sang K. Lee, Kyoung J. Woo, Kee K. Koo,† and Young S. Cho

Division of Chemical Engineering, Korea Institute of Science & Technology, P.O. Box 131, Cheongryang, Seoul 130-650, South Korea, and Department of Chemical Engineering, Sogang University, C.P.O. Box 1142, Seoul 100-611, South Korea

Received July 22, 1998. Revised Manuscript Received October 6, 1998

$BaTiO_3$ particles of ultrafine size and high crystallinity were produced by a spray−coprecipitation technique. To improve stability, titanium isopropoxide was acylated using acetic acid. The sol solutions were prepared by mixing the titanium acylate with aqueous barium acetate . Spray−precipitation was performed in concentrated KOH solution (pH > 13). Investigated variables were the metal content and Ba/Ti ratio in sol solutions, the reaction temperature and time, and the calcination temperature. $BaTiO_3$ particles were synthesized in an aggregate form composed of tiny spherical, crystalline grains (20−30 nm in diameter). The barium-deficient stoichiometry of resulting particles was closely related to a rather poor precipitation yield of barium ions in KOH solution. Crystalline $BaTiO_3$ phase was formed by two different mechanisms: ion−solid reaction and solid-state reaction. $BaTiO_3$ particles, in purely cubic phase as synthesized, underwent a phase transition to tetragonal phase by calcination over 500 °C.

I. Introduction

Barium titanate ($BaTiO_3$) have been used as a primary ferroelectric material for multilayer ceramic chip capacitors (MLCC). Even though $BaTiO_3$ powders were prepared first by the solid-state reaction between $BaCO_3$ and TiO_2,[1] there are generally a variety of methods by which nanosized powders can be produced.[2−4] Nowadays, several brands of commercial $BaTiO_3$ powders are being manufactured by the hydrothermal route.

Enormous efforts have been devoted to develop a powder synthesis process at a reduced temperature. Among many advantages are lower production cost and smaller grain-sized particles. A well-known approach to lower the synthesis temperature of $BaTiO_3$ is to use more reactive precursors. Hydrothermal reactions using amorphous hydrous Ti gel (TiO_2-xH_2O) obtained upon a neutralization reaction of $TiCl_4$ have been studied.[5] Recently, it was reported that organic chelating agents such as acetylacetonate and acetate are used to control the hydrolysis and condensation of alkoxides in the sol−gel method.[6−8] The acetylacetonate was used in the hydrothermal synthesis of $BaTiO_3$.[9]

A conventional pH-based Pechini method was used to prepare $BaTiO_3$ powders.[10] Chandler et al.[11] reported their novel single-component route to produce several ceramic powders of the perovskite structure. Lyons et al.[12] examined the spray−pyrolysis method to produce multicomponent ceramic powders including $BaTiO_3$. A similar technique was employed to produce spherical $BaTiO_3$ powders using two different atomizer types, twin fluid and ultrasonic.[13] The ethanol−water solution of $BaCl_2$ and $TiCl_4$ salts was sprayed prior to pyrolysis at 700 and 900 °C.

Tetragonal $BaTiO_3$ particles were synthesized by a microwave-heating hydrothermal method without sintering at elevated temperatures.[14,15] It was shown that the microwave synthesis has advantages in terms of shortened crystallization time, i.e., increased c/a ratio, enhanced efficiency of postsintering correlated with the increased c/a ratio, over the synthesis based on conventional heating. A physicochemical model for the kinetics

* Corresponding author; gjchoi@dns.kist.re.kr.
† Sogang University.

(1) Galagher, P. K.; Thompson, J. *J. Am. Ceram. Soc.* **1965**, *48* (12), 644.
(2) Ring, T. A. *Fundamentals of Ceramic Powder Processing and Synthesis*; Academic Press: San Diego, **1996**.
(3) Segal, D. *Materials Science and Technology*; Cahn, R. W., Hassan, P., Kramer, E. J., Ed.; VCH: Weinheim, 1996; Vol. 17A, Chapter 3.
(4) Brinker, C. J.; Scherer, G. W. *Sol−Gel Science: The Physics and Chemistry of Sol−Gel Processing*; Academic Press: San Diego, 1990.
(5) Pfaff, G. *J. Eur. Ceram. Soc.* **1991**, *8*, 35.
(6) Livage, J. In *Chemical Processing of Ceramics*; Lee, B. I., Pope, E. J. A., Ed.; Marcel Dekker: New York, 1994; p 3.
(7) Livage, J.; Sanchez, C.; Henry, M.; Doeuff, S. *Solid State Ionics* **1989**, *32/33*, 633.
(8) Phule, P. P.; Risbud, S. H. *Mater. Sci. Engng.* **1989**, *B3*, 241.
(9) Moon, J. Ph.D. Dissertation, University of Florida, 1996.
(10) Kumar, S.; Messing, G. L. *Mater. Res. Soc. Symp. Proc.* **1992**, *271*, 95.
(11) Chandler, C. D.; Hampden-Smith, M. J.; Brinker, C. J. *Mater. Res. Soc. Symp. Proc.* **1992**, *271*, 89.
(12) Lyons, S. W.; Ortega, J.; Wang, L. M.; Kodas, T. T. *Mater. Res. Soc. Symp. Proc.* **1992**, *271*, 907.
(13) Milosevic, O. B.; Mirkovic, M. K.; Uskokovic, D. P. *J. Am. Ceram. Soc.* **1996**, *79* (6), 1720.
(14) Ming, Y.; Vileno, E.; Suib, S. L.; Dutta, P. K. *Chem. Mater.* **1997**, *9*, 3023.
(15) Asiaie, R.; Zhu, W.; Akbar, S. A.; Dutta, P. K. *Chem. Mater.* **1996**, *8*, 226.

10.1021/cm980520h CCC: $15.00
Published on Web 12/01/1998

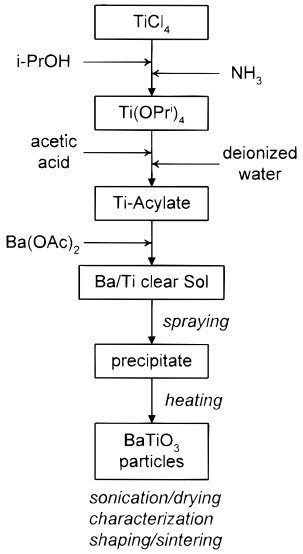

Figure 1. Flow diagram of the whole powder production process.

of $BaTiO_3$ formation from Ba, Ti organometal precursors has been reported.[16]

The principal objective of this study was to produce high-purity, nanosized $BaTiO_3$ particles by a spray−precipitation method. Mechanisms of crystalline $BaTiO_3$ formation were also investigated.

II. Experimental Section

Synthesis of $BaTiO_3$. Figure 1 illustrates the flow diagram of the powder synthesis process. The overall process can be divided into four steps: sol preparation, spray−coprecipitation, hydrothermal reaction, and calcination.

The starting precursor, titanium isopropoxide ($Ti(OPr^i)_4$), was synthesized by reaction of $TiCl_4$ (Aldrich Chemical), NH_3 (99.9%; Daehan Gas Co., Seoul, Korea), and 2-propanol (99%; Junsei Chemical). All chemicals were purified prior to use. The detailed synthesis procedure was reported elsewhere.[17] The reaction yield was approximately 70% after a distillation. The titanium acylate precursor was synthesized by reacting $Ti(OPr^i)_4$ (0.04−0.20 mol) with glacial acetic acid at 25 °C for 1 h. The molar ratio of acetic acid to $Ti(OPr^i)_4$, designated as N, was varied from 1 to 7. With moderate agitation and a very slow addition of distilled water, the initially hazy solution turned clear as the partially hydrolyzed titanium acylate was stabilized. Barium acetate (0.04−0.20 mol) was dissolved in 100 mL of deionized water (Milli-Q Plus) and added to the titanium acylate solution. Deionized water was always degassed using a sonicator prior to use to reduce the influence of carbonate ions. The molar ratio of barium acetate to titanium acylate in sol solution, termed as $[Ba/Ti]_{sol}$, was varied from 1 to 2. The Ba−Ti mixture solution was mildly stirred at 25 °C for 30 min under an inert gas atmosphere to make a slightly hazy sol solution.

Sol solutions of approximately 200 mL at various compositions were sprayed (at 25 mL/min) into a KOH solution bath (500 mL, 2 N) at 25 °C using a two-flow nozzle (Spray Systems, PFj2050).[17] Nitrogen was purged into the KOH bath to enhance the mixing. When sprayed sol particles were brought into contact with the KOH solution, they turned hazy immediately, indictating the formation of a cloudy colloidal solution. The stability of the colloidal solutions was greatly altered by their metal contents. For instance, a colloid solution stayed stable overnight at 0.08 mol of metal content, whereas it formed heavy precipitates on the bottom of the flask within 30 min at 0.2 mol.

The precipitate solution underwent a hydrothermal reaction in a PTFE-lined stainless steel autoclave. Reaction variables were the temperature (80−160 °C) and the time (5 min to 5 h). After reaction, the particle solution was centrifuged (Vision Scientific Co., Seoul, Korea) at 8000 rpm and washed two or three times using deionized water until the pH of the final filtrate became low enough.

Particles after water washing were dried overnight at 80 °C in a vacuum oven. Some particles were calcined for 1 h at various temperatures (400−1200 °C) under moisture-free air using a box furnace.

Characterization. Surface morphology of $BaTiO_3$ particles was measured by FE-SEM (Hitachi, S4200). Each specimen was sensitized with Au-sputtering to avoid charging during SEM analysis. The crystalline structure of the $BaTiO_3$ particles was determined by XRD (Shimatzu X-6000; Cu Kα) analysis. FT-IR spectra were obtained using a single beam spectrometer (Nicolet Magna 750). The transmission spectra were collected for disk specimens mixed with KBr. Raman spectra were obtained using (Perkin-Elmer System 2000). Thermogravitational analysis was carried out via a TGA system (TA 2000). Elemental analysis of $BaTiO_3$ powders were performed by AA, ICP, and other analytical techniques. Bright field images and electron diffraction patterns of $BaTiO_3$ particles were obtained via TEM (Philips CM-30).

III. Results

Effect of Spraying on Particle Morphology. Figure 2 shows typical morphologies of $BaTiO_3$ particles synthesized at 120 °C (a) without and (b) with spraying. Particles synthesized without spraying were composed of small grains 30−100 nm in diameter that were heavily agglomerated to form a large body. Those synthesized with spraying, on the other hand, formed secondary aggregates. They were fairly spherical in shape and 100−200 nm in diameter. Each aggregate consisted of many tiny, spherical grains, 20−30 nm in diameter.

Effect of Hydrothermal Reaction Conditions on Particle Characteristics. Figure 3 exhibits the change in XRD patterns with respect to the reaction temperature. For all reactions, metal content and N were fixed at 0.08 mol and 7, respectively, whereas each reaction was executed for 1 h. As-precipitated particles were almost amorphous but showed weak diffraction peaks for the crystalline $BaCO_3$ phase. XRD patterns of particles synthesized at 100, 120 and 160 °C looked alike, except that patterns for the 100 °C sample contained two more peaks at $2\theta = 28$ and 37° than the others. Peaks other than those two exactly correspond to crystalline $BaTiO_3$. The compounds corresponding to these two peaks would be composed of barium, titanium, oxygen, and potassium. A reasonably good match with JCPDS data, however, was not found. Those two peaks diminished completely when the hydrothermal reaction was performed over 120 °C. The peak intensity for $BaTiO_3$, which is closely related to crystallinity, increased as the reaction temperature was raised to 120 °C. Over 120 °C, however, a significant increase in crystallinity was not observed.

A commercial brand of $BaTiO_3$ particles, known as hydrothermally synthesized, was measured by XRD and compared to our sample. There was no appreciable difference in peak area between them, which indicates that the crystallinity and the purity of as-synthesized

(16) Kumar, S.; Messing, G. L. *J. Am. Ceram. Soc.* **1994**, *77* (11), 2940.

(17) Choi, G. J. Research Report BSV00080-008-1, KIST, Seoul, 1997.

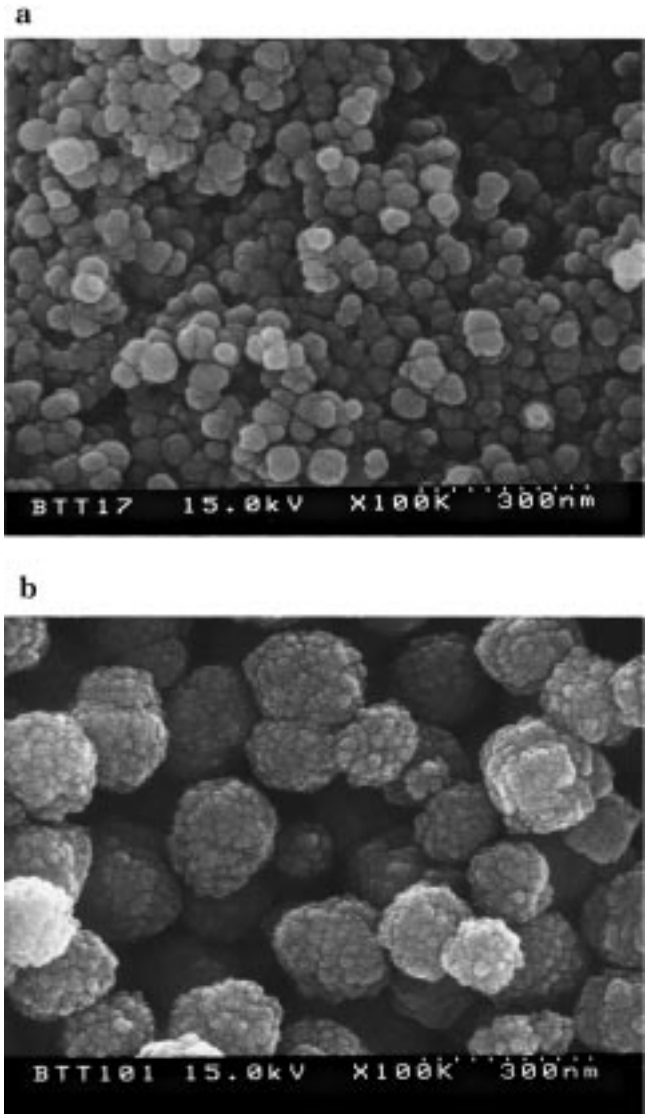

Figure 2. SEM micrographs of typical $BaTiO_3$ particles: (a) nonsprayed and (b) sprayed

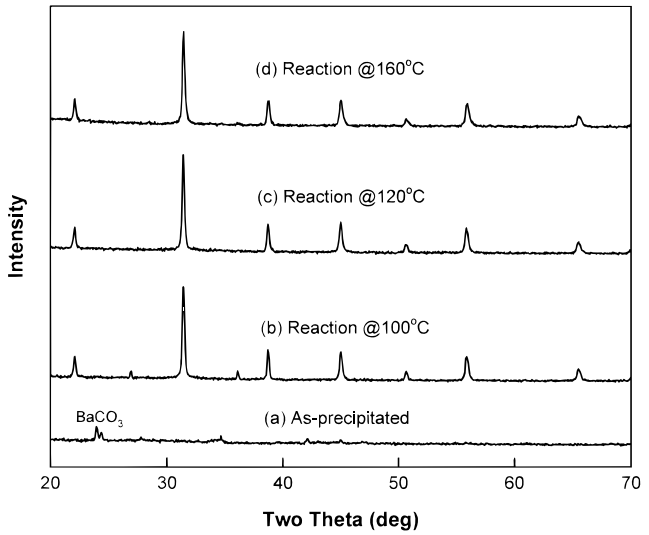

Figure 3. XRD patterns of $BaTiO_3$ particles: (a) as-precipitated and after hydrothermal reaction for 1 h at (b) 100, (c) 120, and (d) 160 °C.

particles are comparable to the commercial $BaTiO_3$ particles.

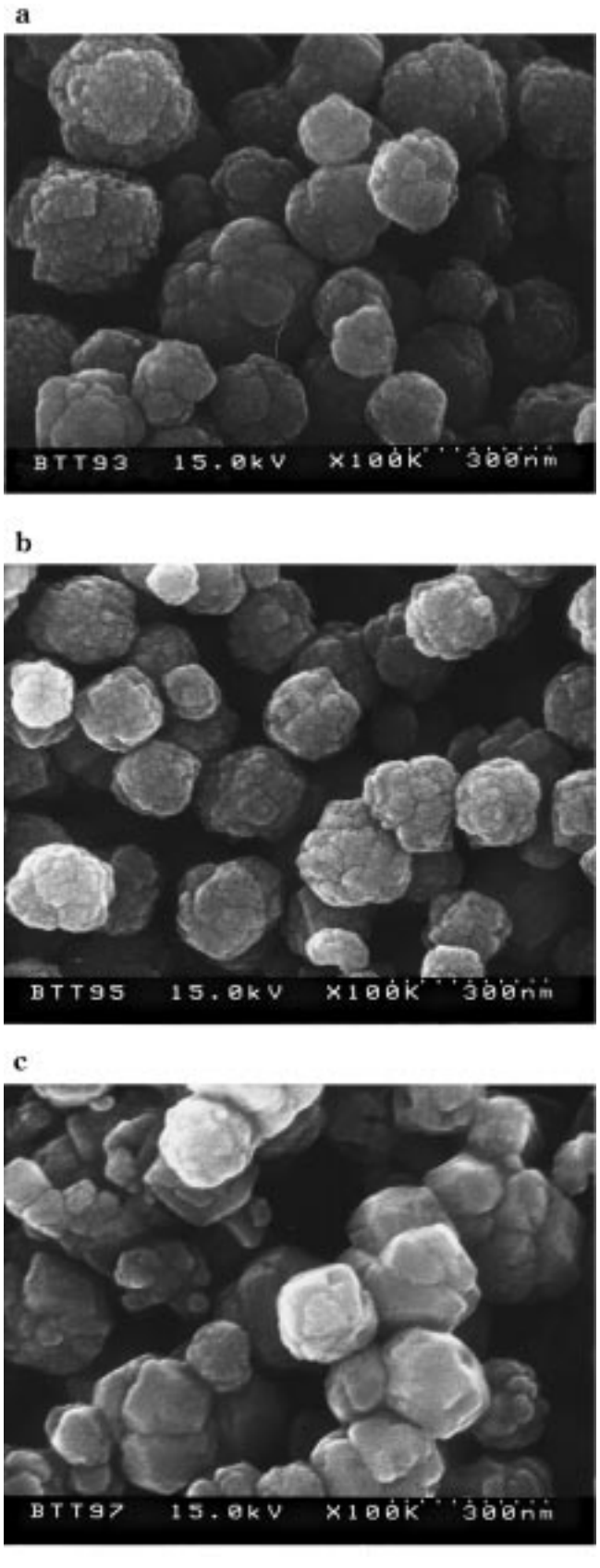

Figure 4. SEM micrographs of $BaTiO_3$ particles after hydrothermal reaction for 1 h at (a) 100, (b) 120, and (c) 160 °C.

SEM micrographs of $BaTiO_3$ particles synthesized at various reaction temperatures are shown in Figure 4. Each micrograph was obtained at 100 000 times magnification, practically the upper limit of the instrument

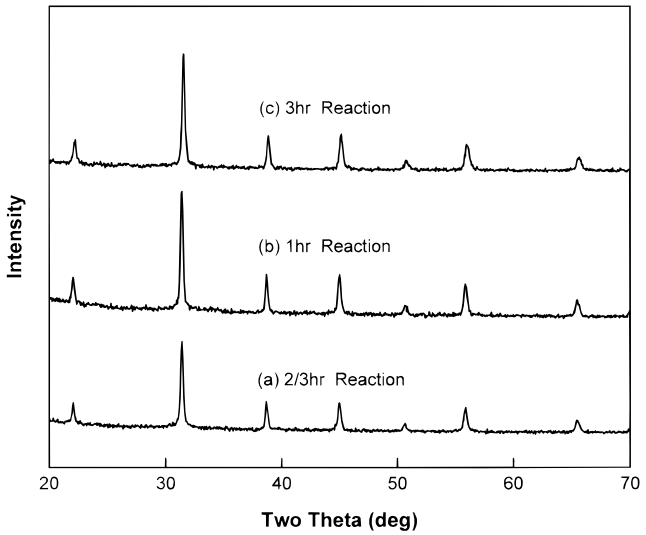

Figure 5. XRD patterns of $BaTiO_3$ particles after hydrothermal reaction at 120 °C for (a) 40 min, (b) 1 h, and (c) 3 h.

at KIST. All $BaTiO_3$ particles had a typical morphology, spherical aggregates composed of many tiny grains 20−30 nm in diameter. One thing to note was that the grain size of particles synthesized at 160 °C was noticeably larger (∼100 nm) than that prepared at 100 or 120 °C. Combining SEM results with XRD data, the optimal temperature for hydrothermal reaction appears to be ∼120 °C.

Figure 5 shows the effect of reaction time at 120 °C on the XRD pattern of $BaTiO_3$ particles. There were no other peaks than those corresponding to crystalline $BaTiO_3$. In terms of peak intensity, 40 min seems insufficient for the reaction to complete at 120 °C. An extended reaction time over 1 h was not as effective in increasing the crystallinity.

Figure 6 illustrates SEM micrographs of $BaTiO_3$ particles synthesized for various reaction times. Overall, this data set looks very similar to that shown in Figure 4. There was no apparent difference in morphology between particles synthesized for 20 min and 1 h. Particles after 3 h reaction, however, contained grains of enlarged size (∼100 nm). Combining XRD results with SEM data, the optimal time for hydrothermal reaction seems to be 1 h.

The plot in Figure 7 summarizes the effect of metal content, when $[Ba/Ti]_{sol}$ was 1, on the aggregate size and grain size. All reactions were performed at 120 °C for 1 h. Sizes were determined using SEM micrographs. Overall, the aggregates became substantially larger (100−240 nm) as the solid content was increased (0.04−0.16 mol). On the other hand, the grain size remained almost constant at 20−30 nm. Besides, no remarkable variation in XRD pattern with respect to the metal content was observed. A higher metal content in sprayed droplets would lead to a smaller distance between precipitates (of the same size), which consequently facilitates the aggregation of grains.

Figure 8 shows a typical TEM bright field image and electron diffraction pattern of $BaTiO_3$ particles synthesized at 120 °C for 1 h. Most aggregates whose diameter ranged from 100 to 200 nm were spherical, in a good agreement with previous SEM results. Each aggregate contains a large number of regions with different contrast. Each region represents an individual grain or group of grains with close orientation. The diffraction pattern indicates that $BaTiO_3$ particles are polycrystalline of rather weak intensity.

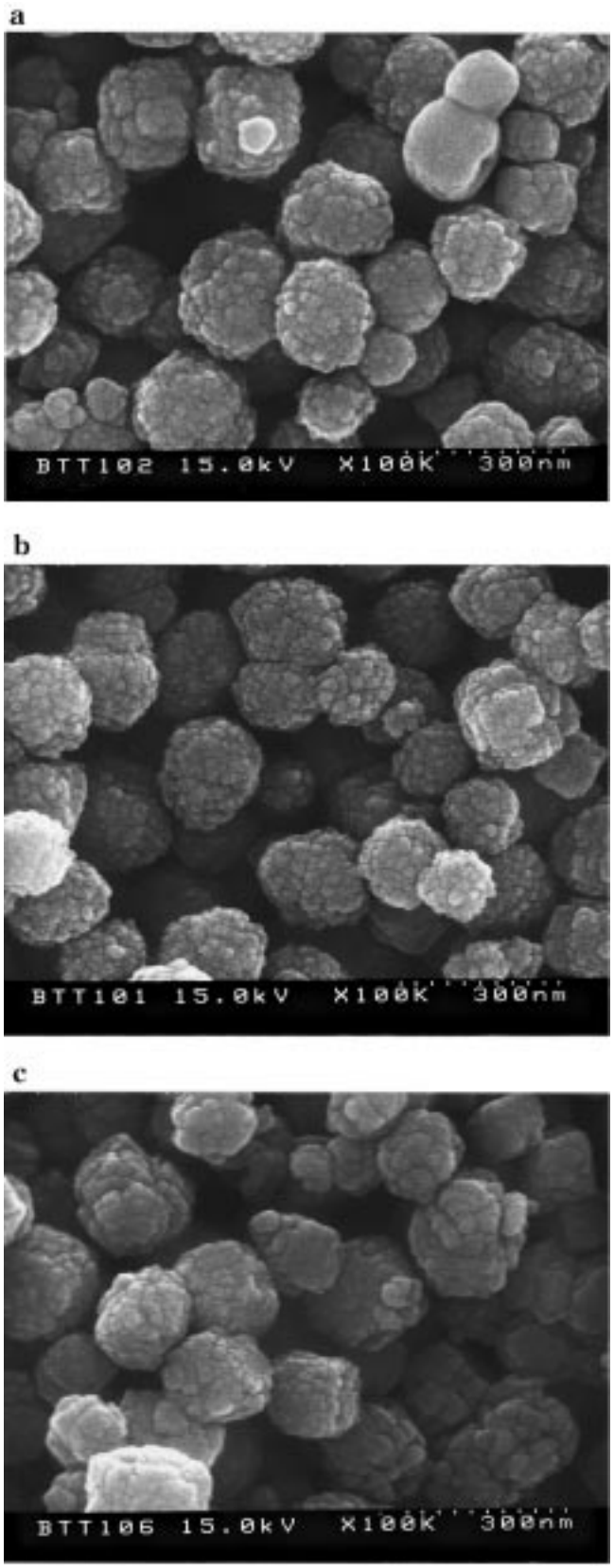

Figure 6. SEM micrographs of $BaTiO_3$ particles after hydrothermal reactions at 120 °C for (a) 40 min, (b) 1 h, and (c) 3 h.

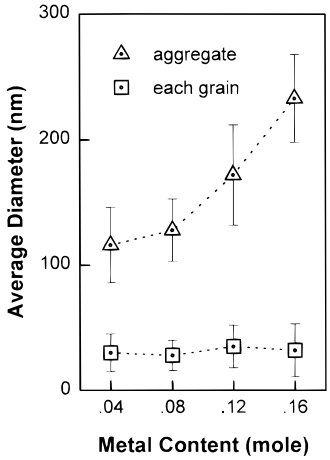

Figure 7. Plot of aggregate and grain sizes versus metal content in sol solution.

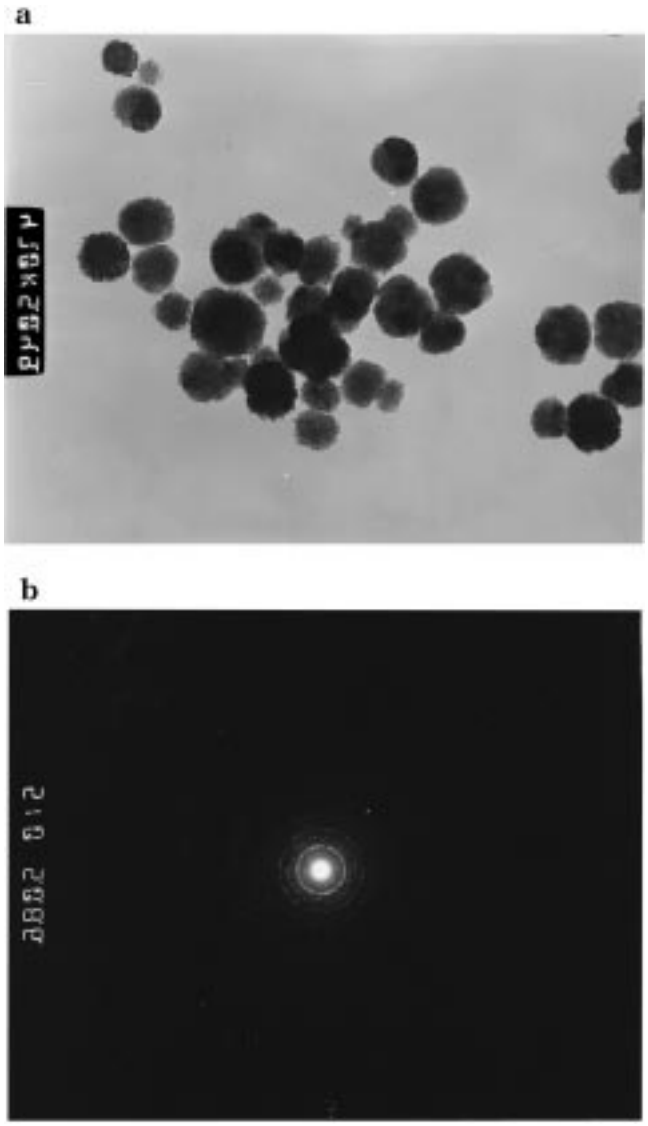

Figure 8. TEM micrographs of typical $BaTiO_3$ particles synthesized at 120°C: (a) bright field image and (b) electron diffraction

Figure 9 illustrates typical TGA results of the commercial and as-synthesized $BaTiO_3$ particles. The TG curve of the commercial powder abruptly goes down in the 300−400 °C region, while it decreases very slowly over 400 °C to reach 98.2% at 1200 °C. On the other hand, the TGA curve of as-synthesized particles decreases substantially in 200−500 °C region. Above 500 °C, it moves down slowly to retain 96.9% of its initial weight at 1200 °C.

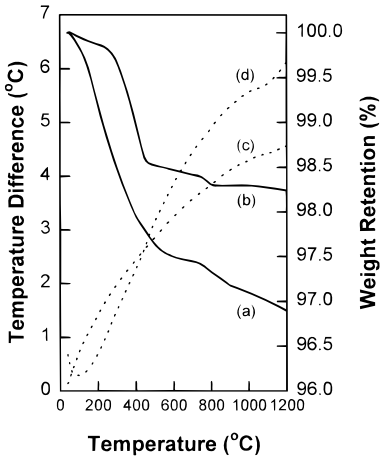

Figure 9. Typical TGA spectra of the commercial and the as-synthesized $BaTiO_3$ particles.

Table 1. Elemental Analysis Results of As-Synthesized $BaTiO_3$ Particles

$[Ba/Ti]_{sol}$	$[Ba/Ti]_{pow}$	carbon (wt %)	OH/Ti ratio in particles
1.0	0.843	0.32	0.707
2.0	0.932	0.30	0.378

As shown in Table 1, $[Ba/Ti]_{sol}$ greatly affected the chemical composition of resulting $BaTiO_3$ particles. As proposed in a series of studies,[8,18] titanium acylate molecules are precipitated in the form of $[(AcO)_XTi(OH)_{4-X}]_n$, which might eventually form a network of [Ti−O−Ti]. When $[Ba/Ti]_{sol}$ was 1, a typical Ba/Ti ratio of particles (designated as $[Ba/Ti]_{pow}$) was 0.843. $[Ba/Ti]_{pow}$ was increased to 0.932 by doubling the $[Ba/Ti]_{sol}$. The carbon content, which is supposedly attributed to the residual carbonate ions, was not changed noticeably by an increase in $[Ba/Ti]_{sol}$.

Another interesting effect of doubling $[Ba/Ti]_{sol}$ was observed in the OH/Ti ratio of as-synthesized $BaTiO_3$ particles. The ratio was greatly decreased from 0.707 to 0.378. Shi et al. suggested that the rather low tetragonality of hydrothermally synthesized particles is closely related to the existence of OH defects in the $BaTiO_3$ crystal structure.[19] Barium-vacancy sites are supposedly occupied with OH, which promotes the development of the metastable cubic phase at room temperature to be a dominant phase in constituting $BaTiO_3$ particles. Nonetheless, neither XRD nor Raman analysis differentiated those two specimens in terms of tetragonality. Two possible explanations can be given for this result: (1) the improved OH/Ti ratio (0.707 → 0.378) by doubling $[Ba/Ti]_{sol}$ was not good enough yet for tetragonality in particles to evolve to a noticeable level, and (2) the tetragonality in particles might not be as closely related to OH defects. The former would be clarified if particles of a much lower OH/Ti ratio could be experimentally produced.

(18) Phule, P. P.; Risbud S. H. In *Ultrastructure Processing of Advanced Materials*; Uhlmann, D. R., Ulrich, D. R., Ed.; John Wiley & Sons: New York, 1992; p 277.

(19) Shi, E.; Xia, C.; Zhong, W.; Wang, B.; Feng, C. *J. Am. Ceram. Soc.* **1997**, *80* (6), 1567.

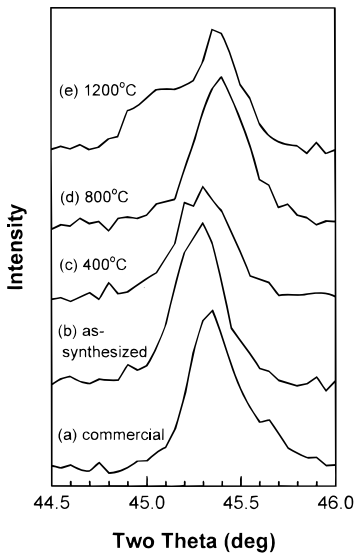

Figure 10. XRD patterns of $BaTiO_3$ particles: (a) commercial, (b) as-synthesized at 120 °C, and after calcination at (c) 400, (d) 800, and (e) 1200 °C.

It was found that the use of KOH instead of NaOH for alkaline precipitating solution substantially reduces the residual amount of alkali metal in synthesized $BaTiO_3$ particles after the same number of washing. The residual content of potassium in fully dried particles after washing twice with deionized water was less than 0.004 wt %, much lower than that of sodium (0.08 wt %). It is believed that potassium, due to a larger ion size, was less able to diffuse into the solid phase during the hydrothermal reaction. Accordingly, residual potassium was washed out with rather ease.

Effect of Calcination on Particle Characteristics. Characteristics of synthesized $BaTiO_3$ particles were remarkably changed by calcination at various temperatures. Figure 10 summarizes the variation of XRD patterns as the calcination temperature increases. XRD spectra are compared in the 44.5−46.0° region of 2θ to examine the tetragonality occurring in {200} plane. A substantial change in XRD pattern was not observed until synthesized $BaTiO_3$ particles were calcined at 1200 °C. Particles calcined at 1200 °C had a split peak near $2\theta = 45°$, which implies an apparent transformation form cubic to tetragonal phase. A commercial powder, known as hydrothermally synthesized, showed an XRD pattern very similar to that of as-synthesized particles after calcination at 800 °C.

Figure 11 illustrates the effect of calcination temperature on SEM micrographs of as-synthesized particles. While the aggregate size remained almost constant, grains in each aggregate became larger as particles were thermally treated at higher temperature. After calcination at 400 °C, the grain size was increased to 40−80 nm. When particles were treated at 800 °C, each aggregate appears to be composed of one fully grown single grain. There was no remarkable difference in morphology between particles calcined at 800 and 1200 °C. Again, in terms of SEM morphology, the commercial $BaTiO_3$ particles were very similar to as-synthesized particles after calcination at 800 °C, which is in a good agreement with previous XRD observations.

Figure 12 compares Raman spectra of $BaTiO_3$ particles calcined at various temperatures. The tetragonality of $BaTiO_3$ has been characterized by two peaks near 307 and 710 cm^{-1}. As-synthesized particles and those treated at 400 °C did not have peaks in these regions, which denotes that their tetragonality is extremely low. On the other hand, particles calcined at 800 °C showed a clear peak at ∼307 cm^{-1}, while presenting a rather weak peak at ∼710 cm^{-1}. Hence, the tetragonality of as-synthesized particles was evolved when they were calcined at between 400 and 800 °C. Recent results exhibited that the lowest temperature for the evolution of tetragonality in particles was near 500 °C on the basis of 1 h at the peak temperature. The intensity of those two characteristic peaks was substantially increased when particles were calcined at 1200 °C. Once again, the commercial powder had a Raman spectrum of almost the same shape as that of synthesized particles after calcination at 800 °C.

The effect of calcination temperature on FT-IR spectra is summarized in Figure 13. As-crystallized particles after drying at 80 °C showed two major peak regions at ∼3500 and ∼1500 cm^{-1}. The first peak region is presumably attributed to OH groups, which were derived from water molecules adsorbed in particles and residual hydroxyl groups. The other peak region would correspond to the existence of organic ligands such as ketone and/or carboxyl groups. Drying at 80 °C overnight in a vacuum oven might have been insufficient to completely remove adsorbed water from particles. The peak intensity for OH groups was greatly decreased to almost zero by a calcination at 400 °C. The organic groups, however, were retained to a great extent after 400 °C treatment. Peaks for organic groups thoroughly disappeared when particles were calcined at 800 °C. On the other hand, the commercial powder showed peaks for organic groups.

IV. Discussion

Acylation of $Ti(OPr^i)_4$. A partial acylation of $Ti(OPr^i)_4$ using glacial acetic acid was intended to slow the hydrolysis rate when titanium precursor molecules were in contact with water afterward. It was reported that the acylation substantially reduces the hydrolysis rate of metal alkoxides.[18] The acylation reaction can be equated as below:

$$Ti(OPr^i)_4 + X\text{AcOH} \rightarrow (\text{AcO})_X Ti(OPr^i)_{4-X} + X Pr^iOH$$

The degree of acylation (X) of $Ti(OPr^i)_4$ at various N (moles of acetic acid per unit mole of $Ti(OPr^i)_4$) was determined via NMR analysis. N was varied as 1, 2, 4, and 7. The value of X was approximately 0.8 when N was 1. As N increased up to 4, X gradually raised to 3. There was no appreciable increase in X, however, when N was varied from 4 to 7. Accordingly, it seems that the acylation of $Ti(OPr^i)_4$ proceeds, not as an irreversible reaction, but as an equilibrium reaction.

The acylation of $Ti(OPr^i)_4$ with $N < 4$ gave a less clear sol solution, which consequently led to a reduced shelf life. The reduced clarity of sol solutions was presumably attributed to a partial gelation of titanium-containing molecules. On the other hand, a sol solution prepared at $N = 7$ remained unchanged longer than 2 days. Hence, $Ti(OPr^i)_4$ acylated with $N = 7$ was used for powder preparation throughout this study.

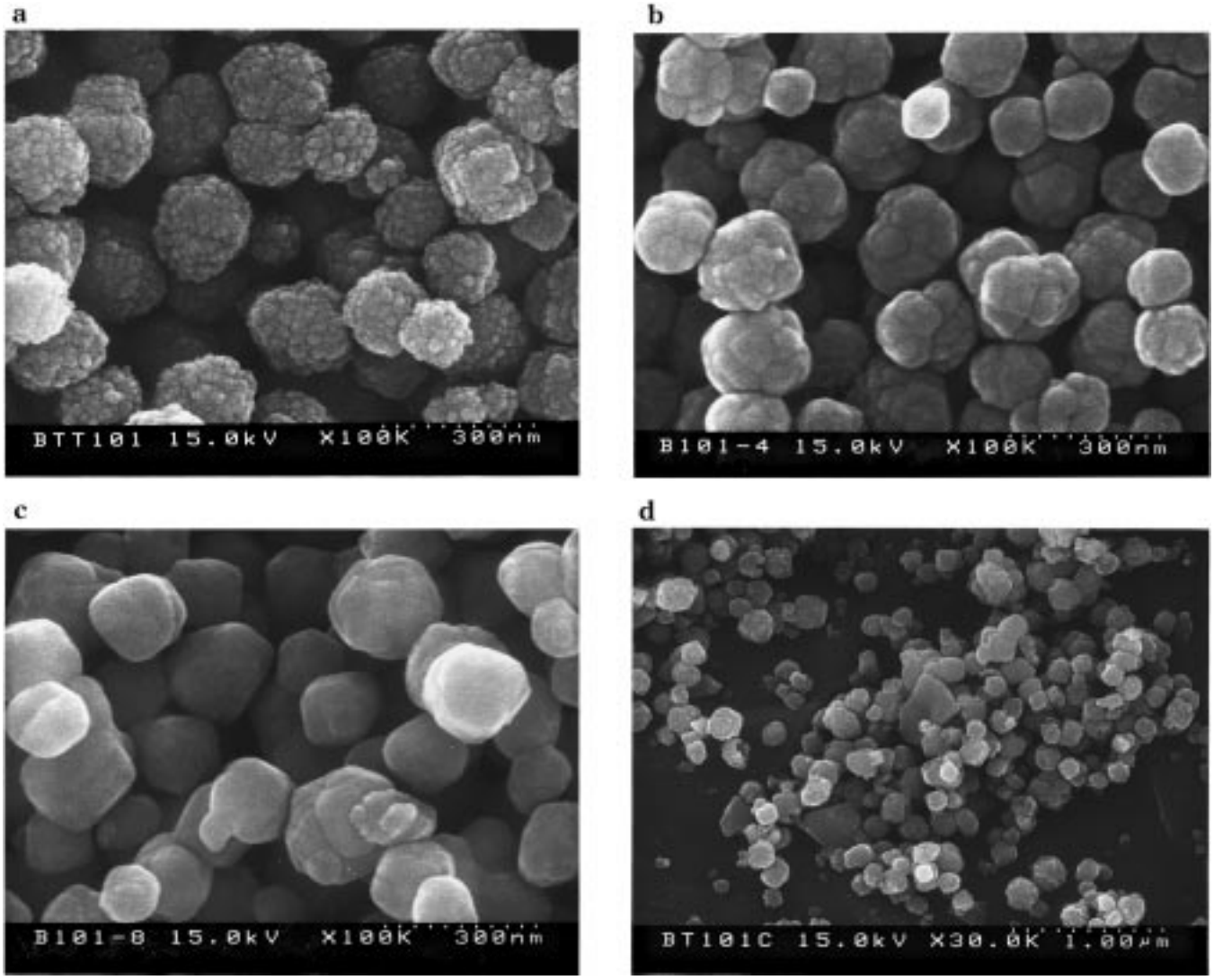

Figure 11. SEM micrographs of $BaTiO_3$ particles: (a) as-synthesized at 120°C and after calcination at (b) 400, (c) 800, and (d) 1200 °C.

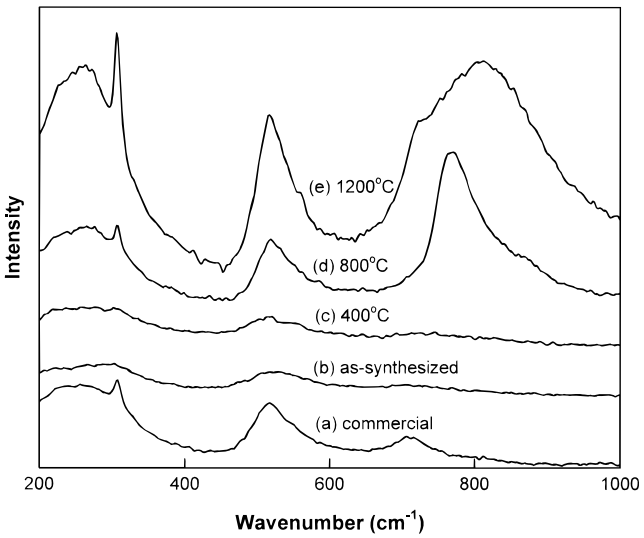

Figure 12. Raman spectra of $BaTiO_3$ particles: (a) commercial, (b) as-synthesized at 120°C, and after calcination at (c) 400, (d) 800, and (e) 1200 °C.

Provided that AcO ligand is hardly hydrolyzed in water, titanyl acylate molecules could only form dimers through a condensation between two hydroxyl groups as shown below:

$$(AcO)_3Ti(OH) + (HO)Ti(OAc)_3 \rightarrow (AcO)_3Ti{-}O{-}Ti(OAc)_3 + H_2O$$

If this is the case, the sol solution would remain as a clear solution for a long time. In the actual experiment, the sol solution became more viscous and less clear if it was left unused longer than 2 days. This phenomena occurred probably due to the hydrolysis of the AcO group in titanyl acylate molecules.[20] The partial hydrolysis of AcO groups would be accompanied by the three-dimensional networking in titanium-containing molecules, which causes a gelation in the previously clear sol solution.

Spraying and Coprecipitation. When a sol solution was sprayed into concentrated KOH solution, precipitated phases were formed immediately. According to an image analysis, the diameters of the sprayed solution droplets were distributed mostly in the range 15−25 μm (avg diameter = 20 μm). Taking the metal content into

(20) Henry, M.; Jolivet, J. P.; Livage, J. In *Ultrastructure Processing of Advanced Materials*; Uhlmann, D. R., Ulrich, D. R., Ed.; John Wiley & Sons: New York, 1992; p 23

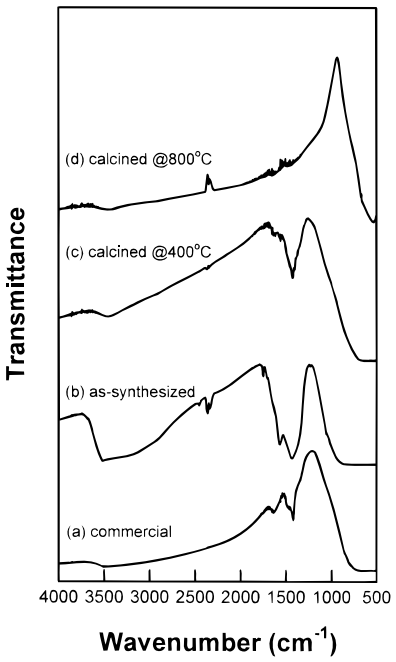

Figure 13. FT-IR spectra of $BaTiO_3$ particles: (a) commercial, (b) as-synthesized at 120 °C, and after calcination at (c) 400 and (d) 800 °C.

account, each liquid droplet of 20 μm in diameter would make a spherical $BaTiO_3$ particle of approximately 2 μm in diameter. This value is about 10−20 times as large as the actual diameter of typical $BaTiO_3$ aggregates (see Figure 2) synthesized with spraying. This calculation implies that the solid portion in each sprayed droplet must have been redistributed in the nitrogen-purged KOH solution bath later to generate much smaller $BaTiO_3$ aggregates via hydrothermal reaction. Hence, the main effect of spraying using a nozzle on particle morphology might be a enhanced mixing. Use a of spraying nozzle with a smaller diameter might be more suitable for attaining a smaller grain size in resulting $BaTiO_3$ particles.

Even though we tried to minimize the effect of airborne CO_2, it was hardly avoided. Coprecipitation in KOH solution is supposedly initiated by the formation of Ti(acylate−hydroxide). Three reactions are supposed to occur in parallel during coprecipitation process as summarized below:[8,18]

$$(AcO)_3Ti(OPr^i) + OH^-(\text{excess}) \rightarrow [(AcO)_xTi(OH)_{4-x}]_n\downarrow + Pr^iOH \quad (0 \le X \le 3)$$

$$Ba^{2+} + 2OH^- \rightarrow Ba(OH)_2\downarrow$$

$$Ba^{2+} + CO_3^{2-} \rightarrow BaCO_3\downarrow$$

The coprecipitation as above would lead to an extremely homogeneous solid-state mixing on a molecular level between barium- and titanium-containing precipitated species. Upon heating for hydrothermal reaction, a large proportion of this mixture was converted into crystalline $BaTiO_3$ particles of fairly small grain size.

Hydrothermal Reaction and Formation of $BaTiO_3$ Crystallites. As shown earlier in Table 1, the addition of more barium, 100% in excess to titanium, resulted in a substantial increased in $[Ba/Ti]_{pow}$ (0.843 → 0.932). Nonetheless, $BaTiO_3$ particles were still barium-deficient. Whether the precipitation yields of barium- and titanium-containing precursor species remained the same under our processing conditions when they were precipitated together in a concentrated KOH solution was examined. For this study, the precipitate solutions (the solution including precipitates) at $[Ba/Ti]_{sol} = 1$ or 2 were filtered with or without hydrothermal reaction. The barium and titanium contents in each liquid filtrate (termed as "1st filtrate") were determined by elemental analysis. The liquid filtrates obtained with water washing afterward, termed as "2nd filtrates", underwent elemental analysis as well. These results are summarized in Tables 2 and 3.

In all cases, the amount of KOH was fixed as 1 mol, i.e., 500 mL of a 2 N solution. According to Table 2, when $[Ba/Ti]_{sol}$ was 1, the precipitation yield of barium ions was less than 72%. Washing of the precipitated phase with deionized water extracted some additional barium to reduce the yield further to 69%. On the other hand, the precipitation yield of titanium always remains near 100%. Doubling $[Ba/Ti]_{sol}$ slightly increased the amount of precipitated barium by a few percent. Nevertheless, the Ba/Ti ratio in the precipitate phase (designated as $[Ba/Ti]_{ppt}$) is still far below 1. Water washing also reduced the yield down to 72.4%. Hence, there was no significant benefit of increasing $[Ba/Ti]_{sol}$ toward an improved Ba/Ti stoichiometry in resulting particles. The rather poor $[Ba/Ti]_{pow}$ should be related to a fairly low precipitation yield of barium ions in KOH solution.

As mentioned previously, barium ions created by the dissolution of barium acetate in water would form precipitates in alkaline solution by the following reaction:

$$Ba^{2+} + 2OH^- \rightarrow Ba(OH)_2\downarrow$$

Especially in the concentrated alkaline solutions of high pH, the precipitation of barium might occur by recombining with acetate ions as outlined below:

$$Ba^{2+} + 2OAc^- \rightarrow Ba(OAc)_2\downarrow$$

The precipitation behavior of barium acetate solution under equivalent conditions (0.08 or 0.16 mol of barium in contact with 1 mol of KOH) was investigated. In each experiment, the precipitated phase was collected using a centrifuge and dried at 120 °C prior to FT-IR and weight analysis. According to comparison of IR spectra of precipitates with those of commercial $Ba(OH)_2 \cdot 8H_2O$, the acetate proportion in the total precipitation of barium ions was not high. Hence, the weight analysis was performed with a reasonable assumption that the precipitate phase is purely composed of $Ba(OH)_2$.

The results are summarized in Figure 14. When the amount of $Ba(OAc)_2$ was 0.08 mol, the precipitation yield was as high as 95%. As the amount of $Ba(OAc)_2$ was increased to 0.16 mol, the precipitation yield of barium ions became lower than 70%. The curve approximately presents the extent of deviation in precipitation yield as the amount of $Ba(OAc)_2$ increases. This result implies that an approach merely to keep increasing the barium content would not work as efficiently for an improved $[Ba/Ti]_{pow}$. Performing the precipitation in a KOH bath

Table 2. Summary of Elemental Analysis for Coprecipitation at 25 °C

	amount, g				amount, g		
species	initially added (mol)	1st filtrate	1st left	1st yield, % (% to Ti)	2nd filtrate	2nd left	2nd yield, % (% to Ti)
Ba	10.986 (0.08)	3.101	7.885	71.8 (71.8)	0.302	7.583	69.0 (69.0)
Ti	3.830 (0.08)	7.1×10^{-5}	3.80	~100	~0	3.830	~100
Ba	21.972 (0.16)	13.267	8.706	39.6 (79.2)	0.862	7.844	35.7 (71.4)
Ti	3.830 (0.08)	8.2×10^{-5}	3.830	~100	~0	3.830	~100

Table 3. Summary of Elemental Analysis for the Hydrothermal Reaction at 120 °C

	amount, g				amount, g		
species	initially added (mol)	1st filtrate	1st left	1st yield, % (% to Ti)	2nd filtrate	2nd left	2nd yield, % (% to Ti)
Ba	10.986 (0.08)	0.918	10.068	91.6 (91.6)	0.028	10.040	91.4 (91.4)
Ti	3.830 (0.08)	4.2×10^{-4}	3.830	~100	~0	3.830	~100
Ba	21.972 (0.16)	10.882	11.091	50.5 (100.9)	0.037	11.054	50.3 (100.6)
Ti	3.830 (0.08)	3.7×10^{-4}	3.830	~100	~0	3.830	~100

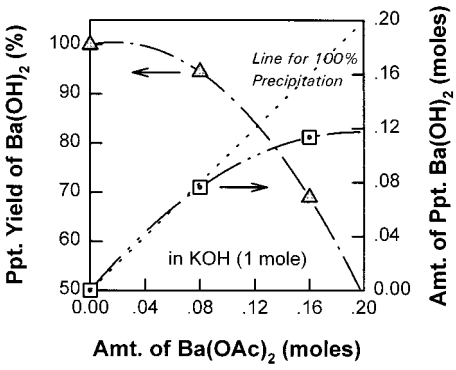

Figure 14. Precipitation curves of $Ba(OAc)_2$ in KOH solution (2 N/500 mL).

of even higher pH could be one feasible method to increase the precipitation yield of barium ions.

According to data in Table 2, when barium ions were coprecipitated with titanium, their precipitation yields (i.e., 1st yield) were 69.0% and 35.7% when $[Ba/Ti]_{sol} = 1$ and 2, respectively. Those values were approximately 25−26% less than those obtained by the sole barium precipitation experiment. The difference should be attributed to the precipitation of titanium-containing sol species. A partial consumption of OH^- by titanium-containing molecules should further reduce the precipitation yields of barium ions. Another possible factor which might have altered the precipitation characteristics is the existence of solvents other than water, such as acetic acid and 2-propanol, in our reaction system.

Table 3 presents the summarized elemental analysis results when the precipitate solutions were heated for the hydrothermal reaction at 120 °C for 1 h. When $[Ba/Ti]_{sol} = 1$, the 1st yield of barium was 91.6%. The yield was increased by nearly 20% via the reaction at 120 °C. The 2nd filtrate included an extremely small amount of barium, which implies that barium ions turned into a compound which was not easily washed off by water. When $[Ba/Ti]_{sol}$ was twice as high, the 1st yield of barium was slightly over 50%, which was high enough for stoichiometric $BaTiO_3$ particles. Similarly, there was no significant loss of barium from synthesized particles by subsequent water washing. When the sol solution went through a precipitation without hydrothermal reaction, the solid mass which survived the filtration contained a large proportion of water-extractable barium compounds. On the other hand, when the precipitate solution underwent a reaction at 120 °C, the barium compounds became much less washable by water.

The conversion yield of barium precursor to $BaTiO_3$ particles was greatly enhanced by reaction at 120 °C. A supplementary experiment was carried out to possibly evaluate a dominant mechanism in the formation of crystalline $BaTiO_3$. Two solid precipitate batches obtained at $[Ba/Ti]sol = 2$, were immersed in xylene (isomers mixed; Junsei Chemical Co.) as a nonpolar solvent. One batch was dried at 120 °C for 1 day to minimize the moisture effect before being mixed with xylene. Both batches underwent (semihydrous and nonhydrous) reactions at 120 °C. Resulting particles were washed using ether and deionized water sequentially to remove residual metal ions and xylene and dried at 120 °C overnight prior to XRD analysis.

XRD patterns of those three specimens are compared in Figure 15. Surprisingly enough, the reaction using dried precipitates in xylene apparently produced crystalline $BaTiO_3$. It was not fully certified, however, whether the moisture effect was thoroughly eliminated by drying at 120 °C for 1 day or not. Nonetheless, the content of residual moisture in precipitates after drying should be extremely low. The reaction in xylene with as-filtered precipitates (without drying) gave particles of greater intensity than that with drying, but of lower intensity than that under fully hydrous conditions.

The above results indicate that crystalline $BaTiO_3$ is created primarily by two parallel mechanisms: (1) by ion−solid reactions between barium ions and titanium-containing precipitated phases and (2) by solid-state reactions between precipitate phases containing barium and titanium. Provided that the acylation number of $Ti(OPr^i)_4$ is 3, the equation for ion−solid reaction is proposed as below:

$$[(AcO)_3Ti(OH)]_n(s) + Ba^{2+} + 2OH^- \rightarrow BaTiO_3(s) + 3AcOH$$

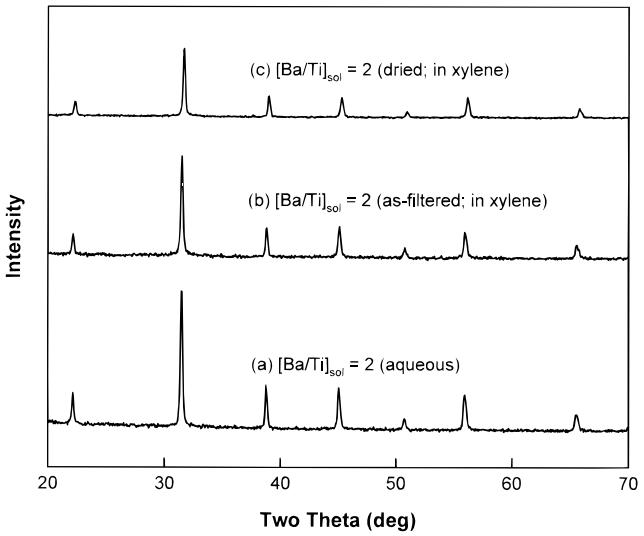

Figure 15. XRD patterns of $BaTiO_3$ particles synthesized at 120 °C with $[Ba/Ti]_{sol} = 2$: (a) hydrous, (b) semihydrous, and (c) nonhydrous conditions.

The solid-state reaction for $BaTiO_3$ formation at 120 °C might be equated as below:

$$[(AcO)_3Ti(OH)]_n(s) + Ba(OH)_2(s) \rightarrow BaTiO_3(s) + 3AcOH$$

Mixing on a molecular level between barium- and titanium-containing molecules when spray-precipitation was performed seems to enable the solid-state reaction to occur, even at low temperatures such as 120 °C. Considering that a greater concentration of barium ions gave a greater contribution for additional $BaTiO_3$ formation, the whole process of the latter route appears to be controlled by the diffusion of barium ions.

A rough comparison of those diffraction peaks in Figure 15, in terms of intensity, seems to suggest that neither mechanism is dominant in the formation of crystalline $BaTiO_3$. Effects from those two routes appear rather similar. More explicit explanation will require a further study in reaction mechanisms.

Tetragonality and Calcination. According to XRD and Raman results, as-synthesized $BaTiO_3$ particles did not show any tetragonality. It is supposedly attributed to several factors: (1) a high content of hydroxyl group or other impurities in $BaTiO_3$ particles, which make the cubic phase highly stable at room temperature and (2) small crystallite size which restricts the stabilization of tetragonal phase by interfacial strain with adjacent grains. As-synthesized $BaTiO_3$ particles, based on elemental analysis results, are believed to contain OH group to a great extent (typically OH/Ti > 0.37 in particles). The tetragonality of $BaTiO_3$ particles evolved upon calcination over 500 °C and gradually increased by heating at higher temperature. Since such a thermal treatment causes grain growth as well as elimination of OH defects, the mechanism for tetragonality evolution would be explained with those two factors combined.

V. Conclusions

Through acylation with excess acetic acid, $Ti(OPr^i)_4$ was stabilized against rapid hydrolysis and rendered suitable for sol processing. According to FT-IR analysis, titanium-containing molecules in sol solution were precipitated in hydroxide form when sprayed in concentrated KOH solution. A Ti−O−Ti network might be formed during hydrothermal reaction at elevated temperatures.

Several variables were examined such as the metal content and Ba/Ti ratio in sol solution, the reaction temperature and time, and the calcination temperature. $BaTiO_3$ particles of high crystallinity and 20−30 nm in grain size were synthesized by hydrothermal reaction at 120 °C for 1 h. A longer reaction time or a higher temperature gave $BaTiO_3$ particles of larger grain size. Synthesized particles, however, were barium-deficient with a typical Ba/Ti ratio ∼0.85. The addition of barium in 100% excess to titanium in sol solutions resulted in a slight increase of Ba/Ti ratio in particles, typically ∼0.94. It was found that the low efficiency of excess barium for improvement in stoichiometry is mainly attributed to a rather low precipitation yield of barium ions in KOH solution.

Reactions of dried precipitates under nonhydrous conditions using xylene as a solvent also produced crystalline $BaTiO_3$. Particles synthesized in xylene, however, had substantially lower crystallinity than those produced under hydrous conditions. Accordingly, it seems that crystalline $BaTiO_3$ is formed by two different mechanisms: by reaction between barium ions and Ti-containing precipitates and by solid-state reaction between Ba- and Ti-containing precipitated phases.

As-synthesized particles were mostly of cubic phase. Their low tetragonality is supposedly attributed to two factor: (1) high OH content and (2) small crystallite size (20−30 nm). $BaTiO_3$ particles of tetragonal phase were obtained when they were calcined over 500 °C. The increased tetragonality upon calcination was attributed to the reduction of the OH content as well as the grain growth in $BaTiO_3$ particles.

Acknowledgment. This research has been conducted under the KIST-2000 program sponsored by the Minister of Science and Technology in Korea. We greatly appreciate Dr. Hoon. S. Kim and Dr. Dong Y. Kim for their assistance on XRD and Raman analysis, respectively.

CM980520H